Dispersion of Homogeneous and Inhomogeneous Waves in the Yee Finite-Difference Time-Domain Grid

John B. Schneider, *Member, IEEE,* and Robert J. Kruhlak

***Abstract*—The numerical dispersion relation governing the propagation of homogeneous plane waves in a finite-difference time-domain (FDTD) grid is well known. However, homogeneous plane waves, by themselves, do not form a complete basis set capable of representing all valid field distributions. A complete basis set is obtained by including inhomogeneous waves, where, in the physical world, constant phase planes must be orthogonal to constant amplitude planes for lossless media. In this paper, we present a dispersion analysis for both homogeneous and inhomogeneous plane waves in the Yee FDTD grid. We show that, in general, the constant amplitude and constant phase planes of inhomogeneous plane waves are not orthogonal, but they approach orthogonality for fine discretization. The dispersion analysis also shows that, for very coarsely resolved fields, homogeneous waves will experience exponential decay as they propagate and they may propagate faster than the speed of light. Bounds are established for the speed of propagation within the grid, as well as the highest frequency and the shortest wavelength that can be coupled into the grid. Analysis is restricted to the classic Yee algorithm, but a similar approach can be used to analyze other time-domain finite-difference methods.**

***Index Terms*—FDTD methods.**

I. Introduction

THE second-order Yee finite-difference time-domain (FDTD) technique [1] is arguably the most robust and successful numerical technique available today to solve problems in electromagnetic-wave propagation. The technique has been the subject of three books [2]–[4], as well as nearly 3000 journal and conference papers [5], [6]. Despite the vast attention the FDTD method has received, the dispersion relation for the complete plane-wave basis set has never been derived. Rules-of-thumb have been developed for suitable discretizations (e.g., [7]). However, these rules have been based solely on consideration of homogeneous (propagating) waves and may not be useful when inhomogeneous (evanescent) fields play a significant role in a given problem.

Taflove has previously derived the dispersion relation for homogeneous waves in the FDTD grid [8] (see also [3]). The equation he derived is correct, but the assumption that some coarsely resolved fields have a phase velocity of zero is not. As Taflove reported, the phase velocity decreases as the discretization becomes more coarse. However, as was shown in [9], a threshold eventually is reached beyond which a further increase in the coarseness results in a wavenumber that is complex. The phase velocity for these waves with complex wavenumbers actually increases with grid coarseness and at no point is it zero. In fact, certain spectral components, which we refer to as superluminal, have a phase velocity greater than the speed of light. One-dimensional (1-D) (or grid-aligned) superluminal FDTD propagation was explored in [9]. The analysis demonstrating superluminal behavior in the FDTD grid will be restated in the Section II and results will be given for obliquely propagating waves.

In Section III, we present the dispersion relation for inhomogeneous plane waves (the familiar homogeneous dispersion relation is a special case of the more general inhomogeneous one). We show that the planes of constant phase and constant amplitude are not necessarily orthogonal in a lossless FDTD grid. We also demonstrate how the dispersion relation can be used to determine the attenuation constant associated with total internal reflection in FDTD simulations. This analysis shows how the dispersion relation can be used to quantify the error in evanescent fields. For the case of total internal reflection, it is found that the error in the attenuation constant in the rarer medium is strongly governed by the discretization in the denser medium.

We restrict the analysis to the original Yee algorithm since it is still one of the most popular and robust time-domain finite-difference techniques. Although simulations of real (physical world) wave phenomena are not done near the discretization limit supported by the Yee grid, in nearly all FDTD simulations there will be some energy present in this coarsely resolved portion of the spectrum. Our analysis clearly defines the behavior of the Yee grid at and near the discretization limit for both homogeneous and inhomogeneous wave propagation. Although the Yee algorithm is the focus here, a similar analysis, i.e., one that does not restrict consideration to real wavenumbers, can be applied equally well to other techniques.

II. Homogeneous Waves

In this section, we reexamine the dispersion relation for homogeneous plane waves in the Yee grid. Starting from the familiar FDTD dispersion relation, it is shown that waves with complex wavenumbers are supported by the grid for coarse discretizations. These complex waves attenuate as they propagate

Manuscript received June 7, 1999. This work was supported by the Office of Naval Research, Code 321OA.

J. B. Schneider is with the School of Electrical Engineering and Computer Science, Washington State University, Pullman, WA 99164-2752 USA (e-mail: schneidj@eecs.wsu.edu).

R. J. Kruhlak was with the Nonlinear Optics Laboratory, Department of Physics, Washington State University, Pullman, WA 99164-2814 USA. He is now with the Applied Optics Centre, University of Auckland, Auckland Private Bag 92019, New Zealand.

Publisher Item Identifier S 0018-9480(01)01067-5.

and can, depending on the grid resolution, propagate faster or slower than the speed of light in the physical world. We establish bounds on the greatest propagation speed within the grid, as well as on the highest frequency and the shortest wavelength that can be coupled into the grid. The special cases of propagation along the grid diagonal and propagation along one of the grid axes are used to establish the limiting behavior of the grid. Unlike the analysis presented in [9], which only considered 1-D (grid-aligned) propagation, no restrictions are placed on the angle of propagation.

In the physical world, the free-space dispersion relation is $c = \omega/\beta$, where $c = 1/\sqrt{\mu\epsilon}$ is the speed of light, ω is the frequency, and β is the wavenumber. The dispersion relation for homogeneous waves propagating in the Yee grid is [3], [8]

$$\frac{1}{c^2\Delta t^2}\sin^2\left(\frac{\omega\Delta t}{2}\right) = \frac{1}{\Delta x^2}\sin^2\left(\frac{\tilde{\beta}_x\Delta x}{2}\right) + \frac{1}{\Delta y^2}\sin^2\left(\frac{\tilde{\beta}_y\Delta y}{2}\right) + \frac{1}{\Delta z^2}\sin^2\left(\frac{\tilde{\beta}_z\Delta z}{2}\right) \quad (1)$$

where Δx, Δy, and Δz are the spatial step sizes and Δt is the temporal step size. In (1), the temporal dependence is understood to be $\exp(j\omega n\Delta t)$ and the spatial dependence is given by $\exp(-j\tilde{\boldsymbol{\beta}}\cdot\mathbf{r})$, where $\tilde{\beta}_x$, $\tilde{\beta}_y$, and $\tilde{\beta}_z$ are the x-, y-, and z-components of the numeric wave vector $\tilde{\boldsymbol{\beta}}$, respectively, given by

$$\tilde{\beta}_x = \tilde{\beta}\sin\theta\cos\phi \quad (2)$$

$$\tilde{\beta}_y = \tilde{\beta}\sin\theta\sin\phi \quad (3)$$

$$\tilde{\beta}_z = \tilde{\beta}\cos\theta \quad (4)$$

and $\mathbf{r}$ is the position vector that can only take on the discrete values dictated by the node locations within the Yee grid. In general, a tilde will be used to distinguish between numeric and exact (i.e., physical world) quantities.

In an FDTD simulation, one selects the temporal and spatial step sizes. As time-stepping progresses, one has complete control over the temporal variation of the source functions introducing energy into the grid. Hence, one can establish exact correspondence between the temporal variations in the grid and physical world. However, the phase velocity of any propagating wave is dictated by the grid itself—one cannot establish exact correspondence between wavenumbers in the grid and physical world. Therefore, the frequency ω in (1) is assumed to be exact and does not require a tilde, while the wavenumbers $\tilde{\beta}_x$, $\tilde{\beta}_y$, and $\tilde{\beta}_z$ are not exact and require a tilde.

To simplify the analysis, we assume a uniform grid in which $\Delta x = \Delta y = \Delta z = \delta$. The argument of the left-hand-side sine function in (1) can be expressed in terms of the points per wavelength and the Courant number

$$\frac{1}{2}\omega\Delta t = \frac{1}{2}\frac{2\pi c}{\lambda}\Delta t = \frac{\pi}{N_\lambda}\frac{c\Delta t}{\delta} = \frac{\pi}{N_\lambda}S$$

where $N_\lambda = \lambda/\delta$ is the points per wavelength, λ is the exact wavelength, and $S = c\Delta t/\delta$ is the Courant number (or stability factor). Thus, for a uniform grid, (1) can be written as

$$\frac{1}{S^2}\sin^2\left(\frac{\pi}{N_\lambda}S\right) = \sin^2\left(\frac{\tilde{\beta}_x\delta}{2}\right) + \sin^2\left(\frac{\tilde{\beta}_y\delta}{2}\right) + \sin^2\left(\frac{\tilde{\beta}_z\delta}{2}\right). \quad (5)$$

Equations (2)–(4) can be used in (5) to obtain an expression that relates the numeric wavenumber $\tilde{\beta}$ to the Courant number S, points per wavelength, and direction of propagation. Typically, the numeric wavenumber must be determined from (5) using a root-finding technique since a general closed-form solution does not exist. However, closed-form solutions are permissible in special cases as shown below.

To demonstrate that the numeric wavenumber can be complex and that the phase velocity can be greater than the speed of light, we first consider grid-aligned propagation such that two of the numeric wavenumber components in (2)–(4) are zero and the third is equal to the numeric wavenumber. For example, when the direction of propagation is given by $\theta = \pi/2$, $\phi = 0$, then $\tilde{\beta}_y = \tilde{\beta}_z = 0$ and $\tilde{\beta}_x = \tilde{\beta}$. In this case, the dispersion relation can be solved for the numeric wavenumber to yield

$$\tilde{\beta}_1\delta = 2\sin^{-1}\left(\frac{1}{S}\sin\left(\frac{\pi}{N_\lambda}S\right)\right) = 2\sin^{-1}(\zeta_1) \quad (6)$$

where a subscript one has been added to $\tilde{\beta}$ to indicate this is for grid-aligned propagation and the argument of the arcsine is defined for notational convenience to be $\zeta_1 = \sin(\pi S/N_\lambda)/S$.

In three-dimensional (3-D) simulations, the Courant number S must be less than or equal to $1/\sqrt{3}$ and, hence ζ_1 can be greater than unity. The threshold between wavenumbers that are real and ones that are complex is a ζ_1 of unity. If N_λ is decreased such that ζ_1 is greater than unity, there is no real $\tilde{\beta}_1$ that satisfies the dispersion relation; however, a complex $\tilde{\beta}_1$ does permit a solution. Although $\tilde{\beta}_1$ will be complex, the corresponding wave is not inhomogeneous since the amplitude and phase planes will be parallel. Instead, the complex wavenumber yields a wave that exponentially decays as it propagates (as if the homogeneous wave were propagating in a lossy material).

A second case that permits a closed-form solution for $\tilde{\beta}$ in (5) is propagation along the 3-D grid diagonal (i.e., $\theta = \cos^{-1}(\sqrt{1/3})$, $\phi = \pi/4$) such that $\tilde{\beta}_x = \tilde{\beta}_y = \tilde{\beta}_z = \tilde{\beta}/\sqrt{3}$. Solving (5) for the numeric wavenumber yields

$$\tilde{\beta}_3\delta = 2\sqrt{3}\sin^{-1}\left(\frac{1}{S\sqrt{3}}\sin\left(\frac{\pi}{N_\lambda}S\right)\right) = 2\sqrt{3}\sin^{-1}(\zeta_3) \quad (7)$$

where $\zeta_3 = \sin(\pi S/N_\lambda)/\sqrt{3}S$ and the subscript three is used to indicate propagation along the diagonal of a 3-D grid. As in (6), the argument of the arcsine ζ_3 can be greater than one. When this occurs, the wavenumber $\tilde{\beta}_3$ is complex.

To establish the range of discretizations that will yield complex wavenumbers, we need to determine the minimum wavelength $\lambda_{\min}$ the grid will support. The highest frequency that can

be coupled into an FDTD grid is $f_{\max} = 1/(2\Delta t)$ (a sequence of alternating plus and minus ones has this frequency) implying a minimum wavelength of $\lambda_{\min} = c/f_{\max} = 2c\Delta t$. Dividing $\lambda_{\min}$ by the spatial step size yields the minimum value of N_λ

$$N_{\lambda,\,\min} = 2c\Delta t/\delta = 2S. \tag{8}$$

In 3-D simulations, where stability dictates that S is less than or equal to $1/\sqrt{3}$, the maximum value of $N_{\lambda,\,\min}$ is $2/\sqrt{3} \approx 1.155$. One might expect a discretization of at least two points per wavelength, otherwise the wave apparently is sampled below the spatial Nyquist rate. This seeming paradox is resolved by noting that N_λ is defined in terms of the physical-world free-space wavelength and not the wavelength in the grid. Even when a given frequency is such that the spatial sampling λ/δ is less than two, the energy corresponding to this spectral component is coupled into the grid—it is not spatially aliased into another frequency.

Inserting (8) into (6) or (7) yields the wavenumbers at the highest frequency the FDTD grid supports as follows:

$$\tilde{\beta}_{1,\,\lim}\delta = 2\sin^{-1}\left(\frac{1}{S}\right) \tag{9}$$

$$\tilde{\beta}_{3,\,\lim}\delta = 2\sqrt{3}\sin^{-1}\left(\frac{1}{S\sqrt{3}}\right). \tag{10}$$

In three dimensions, where $S \leq 1/\sqrt{3}$, the argument of the arcsine in (9) is greater than unity, thus, $\tilde{\beta}_{1,\,\lim}$ is clearly complex. In general, $\tilde{\beta}_1$ will be complex for all spectral components that have a resolution $N_{\lambda,\,\min} \leq N_\lambda \leq S\pi/\sin^{-1}(S)$. On the other hand, the argument of the arcsine in (10) will be unity provided S is equal to the 3-D limit of $1/\sqrt{3}$ and at this limit $\tilde{\beta}_{3,\,\lim}$ is real. However, off-diagonal propagation requires fields with complex wavenumbers. Furthermore, if a simulation uses a Courant number below the 3-D limit, $\tilde{\beta}_{3,\,\lim}$ will be complex and complex wavenumbers will exist at all angles.

When the argument of the arcsine function in (6) or (7) is greater than unity, the arcsine can be evaluated as follows. The arcsine function is given by [10]

$$\sin^{-1}(\zeta) = -j\ln\left[j\zeta + \sqrt{1-\zeta^2}\right].$$

Assuming ζ is real and greater than one, the argument of the square root is negative. Thus, the argument of the log function can be written $j\zeta + \sqrt{1-\zeta^2} = j(\zeta + \sqrt{\zeta^2-1})$. This argument is now purely imaginary with a magnitude of $\zeta + \sqrt{\zeta^2-1}$ and a phase of $\pi/2$. Employing the identity $\ln[re^{j\theta}] = \ln[r] + j\theta$, the arcsine can be written

$$\sin^{-1}(\zeta) = \frac{\pi}{2} - j\ln\left[\zeta + \sqrt{\zeta^2-1}\right].$$

For grid-aligned propagation, this yields

$$\tilde{\beta}_1\delta = \pi - j2\ln\left[\zeta_1 + \sqrt{\zeta_1^2-1}\right] \tag{11}$$

where, as before, $\zeta_1 = \sin(S\pi/N_\lambda)/S$. For plane-wave propagation given by $\exp(-j\tilde{\beta}_1\delta I)$, where I is the spatial index, the per-cell phase constant is π and the per-cell attenuation constant is $2\ln[\zeta_1 + \sqrt{\zeta_1^2-1}]$. Note that, provided ζ_1 is greater than one, the phase constant is independent of the discretization.

To compare the numeric and exact phase velocities, we take the ratio of the numeric phase velocity to the exact velocity for grid-aligned and diagonal propagation. The numeric phase velocity is given by $\tilde{c} = \omega/\Re(\tilde{\beta})$, where $\Re(\cdot)$ indicates the real part (this definition holds for any direction of propagation, but the following discussion focuses on either grid-aligned or diagonal propagation). In the physical world, the (exact) phase velocity is related to the wavenumber via $c = \omega/\beta$ and the continuous wavenumber in free space is given by $\beta = 2\pi/\lambda = 2\pi/(\delta N_\lambda)$. Assuming that a wave is so coarsely sampled that it has a complex wavenumber (i.e., that $\Re(\tilde{\beta})\delta = \pi$), upon canceling terms and multiplying numerator and denominator by δ, the ratio of the numeric to the exact phase velocity for grid-aligned propagation is

$$\frac{\tilde{c}_1}{c} = \frac{\omega\Big/\Re\left(\tilde{\beta}_1\right)}{\omega/\beta} = \frac{\beta\delta}{\Re\left(\tilde{\beta}_1\right)\delta} = \frac{2\pi/N_\lambda}{\pi} = \frac{2}{N_\lambda}. \tag{12}$$

Thus, the numeric phase velocity is related to the exact speed of light by

$$\tilde{c}_1 = \frac{2}{N_\lambda}\,c. \tag{13}$$

For propagation along the grid diagonal, similar steps can be followed. For waves with complex wavenumbers, the result is

$$\tilde{c}_3 = \frac{2}{N_\lambda\sqrt{3}}\,c. \tag{14}$$

Using $N_{\lambda,\,\min}$ in (13) and (14) yields the maximum numeric phase velocities in the FDTD grid for grid-aligned and diagonal propagation

$$\tilde{c}_{1,\,\max} = \frac{1}{S}\,c \tag{15}$$

$$\tilde{c}_{3,\,\max} = \frac{1}{S\sqrt{3}}\,c \tag{16}$$

or, using the definition of the Courant number, these bounds on the speed of propagation can be written as

$$\tilde{c}_{1,\,\max} = \frac{\delta}{\Delta t} \tag{17}$$

$$\tilde{c}_{3,\,\max} = \frac{1}{\sqrt{3}}\,\frac{\delta}{\Delta t}. \tag{18}$$

For grid-aligned propagation, (17) dictates that for every time step Δt some energy will propagate to the adjacent cell, which is δ away. Thus, the maximum phase velocity, or inherent "lattice velocity," for grid-aligned propagation is $\delta/\Delta t$. Note that the lattice velocity is completely determined by the discretization chosen and is independent of all other physical parameters (i.e., it does not depend on ϵ or μ). Similarly, (18) is consistent with the fact that it takes three time steps for energy to travel from one corner of a unit cell to the diagonally opposite corner. Since the distance between the corners is $\sqrt{3}\delta$, the lattice velocity in the diagonal direction is $\delta/\Delta t\sqrt{3}$.

Fig. 1 shows the ratio of the numeric phase velocity to the exact phase velocity as a function of the grid resolution (i.e., the size of the spatial step in fractions of a free-space wavelength). The Courant number corresponds to the 3-D limit of

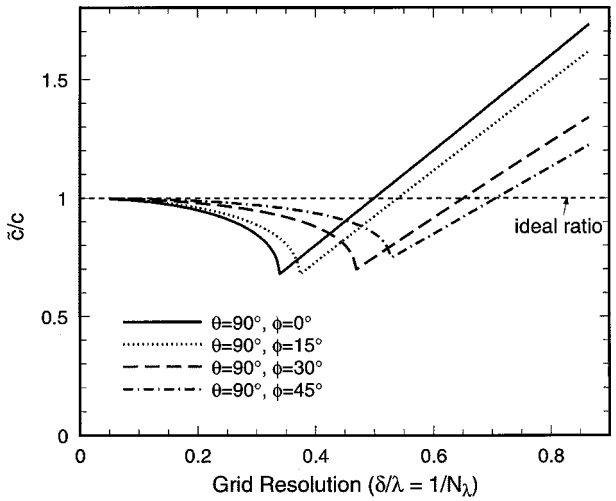

Fig. 1. Ratio of the numeric phase velocity to true phase velocity ($\bar{c}/c$) as a function of grid resolution ($1/N_\lambda$) for four directions of propagation in the xy-plane. The Courant number is $1/\sqrt{3}$, which gives a $N_{\lambda,\min}$ of $2/\sqrt{3} \approx 1.155$ or a maximum spatial step of 0.866λ.

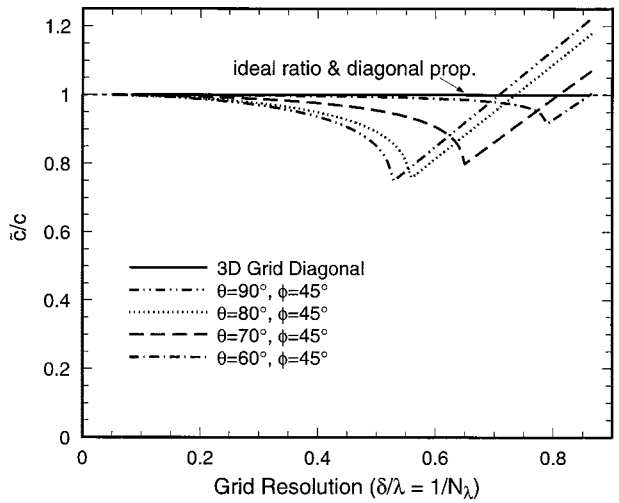

Fig. 2. Ratio of the numeric phase velocity to true phase velocity ($\bar{c}/c$) as a function of grid resolution ($1/N_\lambda$) for five different directions of propagation. For each curve, ϕ is held fixed at 45° while θ takes on the values of 90°, 80°, 70°, or 60°. The result for propagation along the grid diagonal ($\phi = 45°$, $\cos(\theta) = 1/\sqrt{3}$), which overlaps the ideal result, is also plotted. The Courant number is $1/\sqrt{3}$.

$1/\sqrt{3}$ implying a $N_{\lambda,\min}$ of $2/\sqrt{3} \approx 1.155$ or a maximum spatial step size of approximately 0.866λ. Results are shown for four different directions of propagation in the xy-plane, i.e., θ is held fixed at $\pi/2$. The angle ϕ is either 0° (grid-aligned), 15°, 30°, or 45°. The dispersion is symmetric and periodic in ϕ such that results at an angle $\phi = 45° + \xi$ are the same as those at $\phi = 45° - \xi$. Each curve is continuous, but there is a discontinuity in slope, which occurs when the wavenumber transitions from being purely real to complex. Discretizations to the left-hand side of the discontinuity yield purely real wavenumbers.

Fig. 2 is similar to Fig. 1, except ϕ is held constant at 45° and θ takes on the values 90°, 80°, 70°, 60°, or $\cos^{-1}(1/\sqrt{3}) \approx 54.74°$. This last angle corresponds to propagation along the 3-D grid diagonal and produces ideal dispersion since the 3-D Courant limit was used. Had a Courant number less than the limit been used, the phase velocity along the grid diagonal would not be ideal.

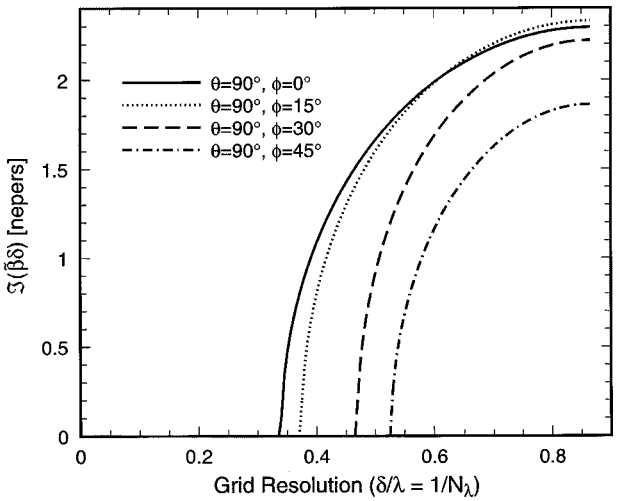

Fig. 3. Per-cell attenuation constant $\Im(\bar{\beta}\delta)$ as a function of grid resolution ($1/N_\lambda$) for four directions of propagation in the xy-plane. The Courant number is $1/\sqrt{3}$.

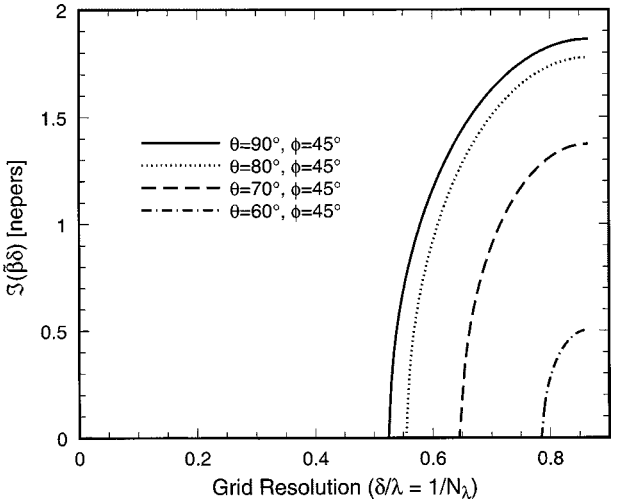

Fig. 4. Per-cell attenuation constant $\Im(\bar{\beta}\delta)$ as a function of grid resolution ($1/N_\lambda$) for four directions of propagation. For each curve, ϕ is held fixed at 45° while θ takes on the values of 90°, 80°, 70°, or 60°. The Courant number is $1/\sqrt{3}$.

Although Figs. 1 and 2 include superluminal waves, the results shown in these figures are consistent with the standard assumption that dispersion error is maximum along the grid axes and is minimum along the diagonals for the Yee FDTD grid. Furthermore, it is still true that dispersion errors are minimum in the Yee algorithm at the Courant limit (i.e., for a fixed angle of propagation, a reduction in the Courant number results in an increase in error).

Figs. 3 and 4 show the "per-cell attenuation constants" as a function of grid resolution for the same directions of propagation considered in Figs. 1 and 2. We define the per-cell attenuation constant as $\Im(\tilde{\beta}\delta)$, where $\Im(\cdot)$ indicates the imaginary part of the argument. The rate of decay typically decreases as the direction of propagation approaches the grid diagonal. There is no attenuation associated with propagation along the grid diagonal ($\theta \approx 54.74°$, $\phi = 45°$).

Since FDTD simulations typically employ a "reasonable" discretization (such as 20 cells per wavelength), it may appear that these waves with complex wavenumbers are mostly of pedagogic interest and may have little practical implications. However, nearly all FDTD simulations start with no energy in the grid. Sources, whether they are embedded within the grid, lining a total-field/scattered-field (TF/SF) boundary, or distributed throughout a scatterer in a SF formulation, must be turned on at some initial time. When these sources turn on, they introduce some energy across the entire spectrum. In a well-designed simulation, the amount of energy at the coarse discretizations will be small, but it is, nevertheless, nonzero. Additionally, there may be other practical reasons for the incorporation of complex wavenumbers into FDTD analysis. For example, it was shown in [9] that the fields at a point in the grid can be predicted from knowledge of the source function and the dispersion relation. It should be possible, therefore, to construct an "exact" TF/SF formulation where there is no leakage of fields across the boundary even when the incident field is propagating obliquely. (Currently, if the incident field is propagating along one of the axes, an exact TF/SF formulation can be obtained using an auxiliary 1-D grid that mimics the dispersion the incident field suffers [11]. However, when the field is obliquely incident, no formulation has been presented that does not leak some energy [3], [12], [13].) As another example, it is rather simple to show that, for complex wavenumbers, the reflection coefficient for the Higdon absorbing boundary condition (ABC) is greater than unity. This growth at the terminal boundary of the grid may explain some aspects of the late-term instability of this ABC.

III. Inhomogeneous Waves

In this section, we obtain the dispersion relation for inhomogeneous waves in the Yee FDTD grid. First, we review the equations governing inhomogeneous waves in the physical world to establish a notational convention. The 2-D FDTD dispersion relation is then derived in the context of a TM^z polarized wave (the magnetic field is transverse to the z-direction). Finally, the dispersion relation governing 3-D propagation is presented and the case of total internal reflection is analyzed.

Consider a wave in the physical world with spatial dependence given by $\exp(-\boldsymbol{\gamma}\cdot\mathbf{r})$, where $\mathbf{r}$ is the position vector (x, y, z) and the complex vector $\boldsymbol{\gamma}$ has components $(\gamma_x, \gamma_y, \gamma_z)$. Let $\boldsymbol{\alpha}$ and $\boldsymbol{\beta}$ be the real and imaginary parts, respectively, of $\boldsymbol{\gamma}$ such that

$$\boldsymbol{\gamma} = \boldsymbol{\alpha} + j\boldsymbol{\beta}. \tag{19}$$

Temporal dependence is understood to be $\exp(j\omega t)$. Note that constant amplitude planes are orthogonal to $\boldsymbol{\alpha}$ and constant phase planes are orthogonal to $\boldsymbol{\beta}$. We subsequently call α the attenuation constant and β is identified as the phase constant. Applying the wave equation to any component of the wave yields, in a source-free region, the following constraint equation:

$$\gamma_x^2 + \gamma_y^2 + \gamma_z^2 - \gamma^2 = 0 \tag{20}$$

or more succinctly

$$\boldsymbol{\gamma}\cdot\boldsymbol{\gamma} - \gamma^2 = 0 \tag{21}$$

where $\gamma^2 = -\omega^2\mu\epsilon + j\omega\mu\sigma$ and σ is the conductivity. Using (19) in (21) and rearranging yields

$$\boldsymbol{\alpha}\cdot\boldsymbol{\alpha} - \boldsymbol{\beta}\cdot\boldsymbol{\beta} + j2\boldsymbol{\alpha}\cdot\boldsymbol{\beta} = -\omega^2\mu\epsilon + j\omega\mu\sigma. \tag{22}$$

Since $\boldsymbol{\alpha}$ and $\boldsymbol{\beta}$ are, by definition, real, the real and imaginary parts of (22) can be equated to obtain

$$\boldsymbol{\beta}\cdot\boldsymbol{\beta} - \boldsymbol{\alpha}\cdot\boldsymbol{\alpha} = \omega^2\mu\epsilon \tag{23}$$

$$\boldsymbol{\alpha}\cdot\boldsymbol{\beta} = \frac{1}{2}\omega\mu\sigma. \tag{24}$$

For a lossless material, the conductivity σ is zero and, thus, (24) dictates that $\boldsymbol{\alpha}$ and $\boldsymbol{\beta}$ are orthogonal, i.e., the constant amplitude planes are orthogonal to the constant phase planes.

One is naturally led to ask if the orthogonality of constant phase and amplitude planes is maintained in the FDTD grid. The answer is no, but they become orthogonal as the grid resolution goes to zero. To derive the dispersion relation for inhomogeneous waves, consider a TM^z plane wave given by

$$E_z(I, J, n) = E_{z0}\exp(j\omega n\Delta t - \tilde{\gamma}_x I\Delta x - \tilde{\gamma}_y J\Delta y) \tag{25}$$

$$H_x(I, J, n) = H_{x0}\exp(j\omega n\Delta t - \tilde{\gamma}_x I\Delta x - \tilde{\gamma}_y J\Delta y) \tag{26}$$

$$H_y(I, J, n) = H_{y0}\exp(j\omega n\Delta t - \tilde{\gamma}_x I\Delta x - \tilde{\gamma}_y J\Delta y) \tag{27}$$

where $\tilde{\gamma}_x$ and $\tilde{\gamma}_y$ are the x- and y-components of the complex numeric wavenumber, I and J are spatial indexes, n is the temporal index, and E_{z0}, H_{x0}, and H_{y0} are amplitudes, only one of which may be set arbitrarily. In the Yee algorithm, the discretized version of the x-component of Faraday's Law is

$$\frac{H_x\left(I, J+\frac{1}{2}, n+\frac{1}{2}\right) - H_x\left(I, J+\frac{1}{2}, n-\frac{1}{2}\right)}{\Delta t} = -\frac{1}{\mu}\frac{E_z(I, J+1, n) - E_z(I, J, n)}{\Delta y}. \tag{28}$$

We assume from the outset that the wave is propagating in a lossless medium. Using the assumed plane wave (25)–(27) in (28) and solving for the ratio of the amplitudes H_{x0} and E_{z0} yields

$$\frac{H_{x0}}{E_{z0}} = -j\frac{\Delta t}{\mu\Delta y}\frac{\sinh\left(\frac{\tilde{\gamma}_y\Delta y}{2}\right)}{\sin\left(\frac{\omega\Delta t}{2}\right)}. \tag{29}$$

An equation similar to (28) can be written for the y-component of Faraday's Law from which one can relate the amplitudes H_{y0} and E_{z0}. The result is

$$\frac{H_{y0}}{E_{z0}} = j\frac{\Delta t}{\mu\Delta x}\frac{\sinh\left(\frac{\tilde{\gamma}_x\Delta x}{2}\right)}{\sin\left(\frac{\omega\Delta t}{2}\right)}. \tag{30}$$

Finally, writing the discrete from of the z-component of Ampere's Law and using (29) and (30) to replace the amplitudes yields

$$\frac{\mu\epsilon}{\Delta t^2}\sin^2\left(\frac{\omega\Delta t}{2}\right) = -\frac{1}{\Delta x^2}\sinh^2\left(\frac{\tilde{\gamma}_x\Delta x}{2}\right) - \frac{1}{\Delta y^2}\sinh^2\left(\frac{\tilde{\gamma}_y\Delta y}{2}\right). \quad (31)$$

We expand $\tilde{\gamma}_x$ and $\tilde{\gamma}_y$ into explicit real and imaginary parts using $\tilde{\gamma}_x = \tilde{\alpha}_x + j\tilde{\beta}_x$ and $\tilde{\gamma}_y = \tilde{\alpha}_y + j\tilde{\beta}_y$. In contrast to the previous section, where (wavenumber) $\tilde{\beta}$ could be complex, in this section, we will restrict consideration to (phase constant) $\tilde{\beta}$'s, which are real. Expanding the $\sinh^2(\cdot)$ terms in (31) and equating the real parts of the left- and right-hand sides yields

$$\frac{\mu\epsilon}{\Delta t^2}\sin^2\left(\frac{\omega\Delta t}{2}\right) = \frac{1}{\Delta x^2}\frac{1}{2}\left[1-\cos\left(\tilde{\beta}_x\Delta x\right)\cosh(\tilde{\alpha}_x\Delta x)\right] + \frac{1}{\Delta y^2}\frac{1}{2}\left[1-\cos\left(\tilde{\beta}_y\Delta y\right)\cosh(\tilde{\alpha}_y\Delta y)\right]. \quad (32)$$

Equating imaginary parts in (31) yields

$$0 = \frac{1}{\Delta x^2}\sin\left(\tilde{\beta}_x\Delta x\right)\sinh(\tilde{\alpha}_x\Delta x) + \frac{1}{\Delta y^2}\sin\left(\tilde{\beta}_y\Delta y\right)\sinh(\tilde{\alpha}_y\Delta y). \quad (33)$$

Equation (32) is the FDTD analog of (23), while (33) is the analog of (24) with a conductivity σ of zero.

The relationship between planes of constant phase and planes of constant amplitude in (lossless) FDTD grids is dictated by (33). Unlike in the physical world, these planes are not necessarily orthogonal. However, employing the small argument approximations for sine and hyperbolic sine, one can write

$$\begin{aligned}&\frac{1}{\Delta x^2}\sin\left(\tilde{\beta}_x\Delta x\right)\sinh(\tilde{\alpha}_x\Delta x) + \frac{1}{\Delta y^2}\sin\left(\tilde{\beta}_y\Delta y\right)\sinh(\tilde{\alpha}_y\Delta y)\\ &= \tilde{\alpha}_x\tilde{\beta}_x\left(1+\left[\tilde{\alpha}_x^2-\tilde{\beta}_x^2\right]\Delta x^2/6\right) + \tilde{\alpha}_y\tilde{\beta}_y\left(1+\left[\tilde{\alpha}_y^2-\tilde{\beta}_y^2\right]\Delta y^2/6\right) + O(\Delta x^4)+O(\Delta y^4).\end{aligned}$$

Thus, the difference between (33) and the exact relation is second order, so that in the limit of small discretization, the constant phase and amplitude planes are orthogonal.

The 3-D version of the inhomogeneous dispersion relation is similar to (32) and (33)—one merely has to add one more term like the ones already appearing on the right-hand side, except

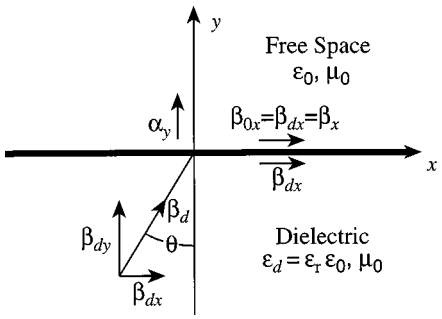

Fig. 5. Assumed geometry for total internal reflection.

z is used instead of x or y. For a uniform grid in which $\Delta x = \Delta y = \Delta z = \delta$, the dispersion relation can be written as follows:

$$\begin{aligned}\frac{2}{S^2}\sin^2\left(\frac{\pi}{N_\lambda}S\right) &= \left[1-\cos\left(\tilde{\beta}_x\delta\right)\cosh(\tilde{\alpha}_x\delta)\right]+\left[1-\cos\left(\tilde{\beta}_y\delta\right)\cosh(\tilde{\alpha}_y\delta)\right]\\ &\quad+\left[1-\cos\left(\tilde{\beta}_z\delta\right)\cosh(\tilde{\alpha}_z\delta)\right] \quad (34)\end{aligned}$$

$$\begin{aligned}0 &= \sin\left(\tilde{\beta}_x\delta\right)\sinh(\tilde{\alpha}_x\delta)+\sin\left(\tilde{\beta}_y\delta\right)\sinh(\tilde{\alpha}_y\delta)\\ &\quad+\sin\left(\tilde{\beta}_z\delta\right)\sinh(\tilde{\alpha}_z\delta). \quad (35)\end{aligned}$$

Equation (34) appears to be different from the familiar FDTD dispersion relation for propagating waves [see (1) or (5)]. However, setting the $\tilde{\alpha}$'s to zero and employing the identity $[1-\cos(\xi)]/2 = \sin^2(\xi/2)$ shows that (34) reduces to the dispersion relation for homogeneous waves.

To illustrate how one might use the dispersion relation to guide the construction of an FDTD simulation, we consider the case of total internal reflection. As shown in Fig. 5, a plane wave is incident from a dielectric to free space. We further assume $\mu_d = \mu_0$, $\epsilon_d = \epsilon_r\epsilon_0$ ($\epsilon_r > 1$), and the incident angle θ is beyond the critical angle.

In the physical world, the magnitude of the phase constant in the dielectric is given by $\beta_d = \omega\sqrt{\epsilon_r\epsilon_0\mu_0} = \sqrt{\epsilon_r}\beta_0$. The x-component of the phase constant is $\beta_x = \beta_d\sin\theta$ and governs the phase propagation tangential to the interface. Continuity of the fields at the interface requires that this phase constant also pertain in the free-space region. When $\beta_d\sin\theta$ is greater than β_0, the fields in the free-space region will be inhomogeneous—constant phase planes will be perpendicular to the x-axis and constant amplitude planes will be perpendicular to the y-axis. The phase and attenuation constants must satisfy the following:

$$\beta_x^2 - \alpha_y^2 = \beta_0^2. \quad (36)$$

Using the x-component of the phase constant, as dictated by the incident field and solving for α_y, yields

$$\alpha_y = \beta_0(\epsilon_r\sin^2\theta - 1)^{1/2}. \quad (37)$$

At the critical angle, α_y is zero and for all angles beyond the critical angle, α_y is real and positive.

In the FDTD grid, we again assume an incident angle of θ that is greater than the critical angle (although, as described below, the precise value of the critical angle will be different in the grid than it is in the physical world). The phase constant in the dielectric is $\tilde{\beta}_d$, which must be obtained via the FDTD dispersion relation. We continue to equate the Courant number S with $c\Delta t/\delta$, where c is the speed of propagation in free space. Therefore, the dispersion relation that pertains in the dielectric should have both S and N_λ scaled by $\sqrt{\epsilon_r}$. Defining $N_{\lambda_d} = N_\lambda/\sqrt{\epsilon_r}$, the (homogeneous) dispersion relation governing $\tilde{\beta}_d$ is

$$\begin{aligned}\frac{\epsilon_r}{S^2}\sin^2\left(\frac{\pi}{N_{\lambda_d}}\frac{S}{\sqrt{\epsilon_r}}\right) &= \sin^2\left(\frac{\tilde{\beta}_{dx}\delta}{2}\right)+\sin^2\left(\frac{\tilde{\beta}_{dy}\delta}{2}\right)\\ &= \sin^2\left(\frac{\tilde{\beta}_d\delta\sin\theta}{2}\right)+\sin^2\left(\frac{\tilde{\beta}_d\delta\cos\theta}{2}\right). \qquad (38)\end{aligned}$$

For a given set of parameters (i.e., ϵ_r, N_λ, S, and θ), (38) can be solved for $\tilde{\beta}_d$ or, more precisely, for $\tilde{\beta}_d\delta\sin\theta$. In free space, the wave is assumed to be inhomogeneous such that $\tilde{\beta}_x > \tilde{\beta}_0$ and $\tilde{\alpha}_x = 0$, i.e., the x-component of the phase constant is nonzero and there is no decay associated with propagation in the x-direction. Thus, the "orthogonality condition" (33) is satisfied in free space provided the y-component of the phase constant is zero. Note that in this limiting (grid-aligned) case the orthogonality condition yields the same behavior as in the physical world—the constant phase and amplitude planes are orthogonal. The attenuation constant $\tilde{\alpha}_y$ must be obtained via (32). Recognizing that continuity of the fields at the interface dictates that the phase constant in the x-direction be the same in both media and using the identity $(1-\cosh(x))/2 = -\sinh^2(x/2)$, $\tilde{\alpha}_y$ is found to be

$$\tilde{\alpha}_y\delta = 2\sinh^{-1}\left(\left[\sin^2\left(\frac{\tilde{\beta}_d\delta\sin\theta}{2}\right)-\frac{1}{S^2}\sin^2\left(\frac{\pi}{N_\lambda}S\right)\right]^{1/2}\right). \qquad (39)$$

Within the FDTD grid, the critical angle can again be defined as the angle at which the attenuation constant $\tilde{\alpha}_y$ is zero, but, rather than (37), this angle must be determined from (39), where $\tilde{\beta}_d\delta\sin\theta$ is obtained from (38).

To facilitate comparison between the physical and discretized worlds, we multiply both sides of (37) by δ to obtain

$$\alpha_y\delta = \beta_0\delta\left(\epsilon_r\sin^2\theta-1\right)^{1/2} = \frac{2\pi}{N_\lambda}\left(\epsilon_r\sin^2\theta-1\right)^{1/2}. \qquad (40)$$

Fig. 6 shows both the exact and FDTD values for $\alpha_y\delta$ as a function of the points per wavelength in free space. We have chosen the dielectric relative permittivity to be nine so that the points per wavelength in the dielectric is one-third of the free-space value. The Courant number is $1/\sqrt{3}$ and the incident angle is either 50°, 70°, or 90°. For each incident angle, the exact solution is shown as a solid line. As would be expected, the agreement between the exact and FDTD values improves as the discretization increases. Note that, as shown in (39), the phase constant in the dielectric is intimately related to the attenuation constant in free space. Since the error in the dielectric phase constant is dictated by the (coarser) sampling within the dielectric, the error in the attenuation constant is governed not so much by the sampling in free space, as by the discretization within the dielectric.

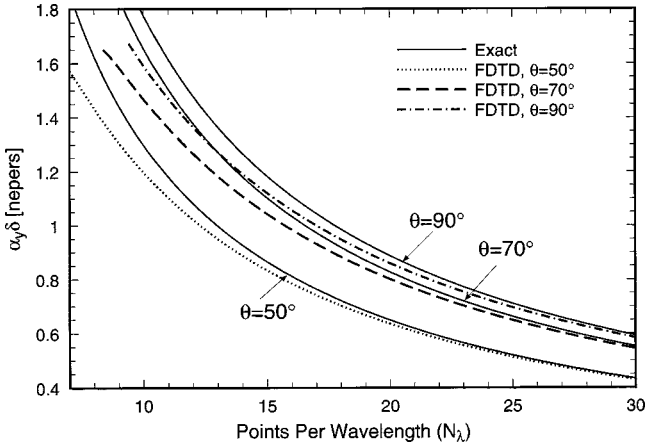

Fig. 6. Attenuation constant $\alpha_y\delta$ as a function of free-space points per wavelength N_λ. The incident angle is 50°, 70°, or 90°. The relative permittivity of the dielectric medium is nine and the Courant number is $1/\sqrt{3}$. The exact solutions are shown as solid lines.

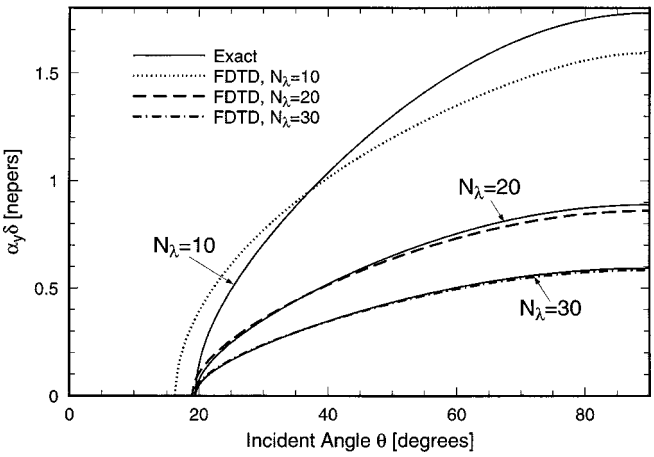

Fig. 7. Attenuation constant $\alpha_y\delta$ as a function of incident angle. The relative permittivity of the dielectric medium is nine and the Courant number is $1/\sqrt{3}$. The points per wavelength is 10, 20, or 30. Exact solutions are shown as solid lines.

Fig. 7 shows the exact and FDTD values for $\alpha_y\delta$ as a function of the incident angle. The relative permittivity and Courant number are the same as Fig. 6 and the points per wavelength is either 10, 20, or 30. For each N_λ, the exact solutions are shown as solid lines. The exact critical angle is approximately 19.47°. All the exact curves, independent of the discretization, go to zero at this angle. The FDTD critical angles, on the other hand, do not correspond to this value. For example, with a discretization of $N_\lambda = 10$, the FDTD critical angle is approximately three degrees less than the exact value (the agreement between the FDTD and exact critical angles is better at the finer discretizations). For $N_\lambda = 10$, one clearly sees that the FDTD attenua-

tion constant can be greater than or less than the exact value depending on the incident angle. This also holds true at the other discretizations.

IV. Conclusion

The FDTD dispersion relation for homogeneous waves permits solutions with complex wavenumbers. These complex waves experience exponential decay as they propagate and they can propagate faster than the speed of light. Consistent with previous assumptions, the dispersion errors associated with these waves are maximum along the grid axes and minimum along the grid diagonal.

The dispersion relation for inhomogeneous plane waves was derived. Unlike in the physical world, the constant amplitude and constant phase planes are not necessarily orthogonal. For the case of total internal reflection, the FDTD grid may introduce too much or too little attenuation, depending on the specific values of the incident angle, relative permittivity, and discretization. Furthermore, the critical angle in the grid will differ from the true critical angle. Using the dispersion relation, it is possible to precisely determine the critical angle and attenuation constant for any given set of parameters.

Acknowledgment

The authors would like to thank E. Forgy, University of Illinois at Urbana-Champaign, for suggesting the term "lattice velocity."

References

[1] K. S. Yee, "Numerical solution of initial boundary value problems involving Maxwell's equations in isotropic media," *IEEE Trans. Antennas Propagat.*, vol. AP-14, pp. 302–307, Mar. 1966.

[2] K. S. Kunz and R. J. Luebbers, *The Finite Difference Time Domain Method for Electromagnetics*. Boca Raton, FL: CRC Press, 1993.

[3] A. Taflove, *Computational Electrodynamics: The Finite-Difference Time-Domain Method*. Norwood, MA: Artech House, 1995.

[4] A. Taflove, Ed., *Advances in Computational Electrodynamics: The Finite-Difference Time-Domain Method*. Norwood, MA: Artech House, 1998.

[5] K. L. Shlager and J. B. Schneider, "A selective survey of the finite-difference time-domain literature," *IEEE Antennas Propagat. Mag.*, vol. 37, pp. 39–56, Aug. 1995.

[6] ——, "A survey of the finite-difference time-domain literature," in *Advances in Computational Electrodynamics: The Finite-Difference Time-Domain Method*, A. Taflove, Ed. Norwood, MA: Artech House, 1998, ch. 1, pp. 1–62.

[7] P. G. Petropoulos, "Phase error control for FD-TD methods of second and fourth order accuracy," *IEEE Trans. Antennas Propagat.*, vol. 42, pp. 859–862, June 1994.

[8] A. Taflove, "Review of the formulation and applications of the finite-difference time-domain method for numerical modeling of electromagnetic wave interactions with arbitrary structures," *Wave Motion*, vol. 10, no. 6, pp. 547–582, 1988.

[9] J. B. Schneider and C. L. Wagner, "FDTD dispersion revisited: Faster-than-light propagation," *IEEE Microwave Guided Wave Lett.*, vol. 9, pp. 54–56, Feb. 1999.

[10] R. V. Churchill, J. W. Brown, and R. F. Verhey, *Complex Variables and Applications*. New York: McGraw-Hill, 1976.

[11] J. Fang, "Time Domain Finite Difference Computation for Maxwell's Equations," Ph.D. dissertation, Elect. Eng. Comput. Sci. Dept., Univ. California at Berkeley, Berkeley, CA, 1989.

[12] U. Oğuz and L. Gürel, "Interpolation techniques to improve the accuracy of the plane wave excitations in the finite difference time domain method," *Radio Sci.*, vol. 32, pp. 2189–2199, Nov.–Dec. 1997.

[13] ——, "An efficient and accurate technique for the incident-wave excitations in the FDTD method," *IEEE Trans. Microwave Theory Tech.*, vol. 46, pp. 869–882, June 1998.

John B. Schneider (M'92) received the B.S. degree in electrical engineering from Tulane University, New Orleans, LA, and the M.S. and Ph.D. degrees in electrical engineering from the University of Washington, Seattle.

He is currently an Assistant Professor in the School of Electrical Engineering and Computer Science, Washington State University, Pullman. His research interests include the use of computational methods to analyze acoustic-, elastic-, and electromagnetic-wave propagation.

Dr. Schneider was the recipient of a 1996 Office of Naval Research Young Investigator Award.

Robert J. Kruhlak received the B.S. degree in math and physics from Northern Michigan University, Marquette, and the M.S. and Ph.D. degrees in physics from Washington State University, Pullman.

He is currently a Research Fellow at the University of Auckland, Auckland, New Zealand. His research interests include experimental and computational investigations of nonlinear optical phenomena.